TIFR/TH/16-31

Portal to non-MSSM models using kinematic edges

Abhishek M. Iyer[1,*] and Ushoshi Maitra[1,†]

[1]*Department of Theoretical Physics, Tata Institute of Fundamental Research, Homi Bhabha Road, Colaba, Mumbai 400 005, India*

Abstract

A heavy Higgs like resonance (H_1) is a characteristic feature of many new physics scenarios beyond the Standard Model (SM). In the event of a discovery it is essential to identify the true nature of underlying theory. In this work we propose a channel, $H_1 \to t_2 t$, where t_2 is a vector-like gauge singlet top-partner that decays into Wb, Zt, ht. We construct different invariant mass distributions which are characterized by the presence of kinematic edges, unique to the topology under consideration. Using these kinematic edges, the masses of the heavy resonances can be extracted upto a reasonable accuracy. Observation of these features are meant to serve as a trigger, thereby mandating a more detailed analysis in a particular direction of parameter space. The absence of these vector-like states in minimal versions of supersymmetric models (MSSM) also serves as a harbinger of such non MSSM-like scenarios.

arXiv:1609.06502v1 [hep-ph] 21 Sep 2016

*Electronic address: abhishek@theory.tifr.res.in

†Electronic address: ushoshi@theory.tifr.res.in

The presence of an elementary scalar in the Standard Model (SM) provides the most compelling reason to expect new physics at the TeV scale and beyond. While new physics candidates may differ quite significantly with respect to the underlying theory, there could be similarities in the properties of the new particles predicted by these scenarios. The most prominent being the presence of a heavy scalar. One class of models (say Class A) which are characterized by these heavy scalars include two Higgs doublet model, supersymmetric model *etc.*. Alternatively, these scalars can also arise as the Kaluza-Klein (KK) excitations of the bulk Higgs in the extra-dimensional models or some minimal extension of Little Higgs scenarios. We refer to these kind of models as Class B. In the event of a discovery of such excited scalars, it is essential to identify the true nature of physics beyond the SM. In this letter we propose an analysis that help us to recognize such distinct features.

The models are segregated into two classes: A and B introduced earlier. The latter is characterized by the presence of additional vector-like fermions. For instance, the vector-like fermions could correspond to the KK excitations of the fermions in the extra dimensional models [1] with the lightest one generally corresponding to the top-partner or they can also arise in the extended Little Higgs model [2, 3]. Using this difference, we attempt to devise a unique signature which is a trademark of models belonging to Class B.

The phenomenology of the heavy top partners at the LHC has been discussed in details in Ref. [4–20]. Similarly the phenomenology of a heavy scalar coming from a general Higgs sector or a warped extra dimension at the LHC has been discussed in Ref. [21, 22]. Recently, ATLAS and CMS have searched for a heavy Higgs-like resonance in the WW^*, diphoton, ZZ and hh channels [23, 24]. Although, translating the maximum observed cross section as an exclusion on the mass of the heavy Higgs is highly model dependent, one can safely assume that a heavy scalar beyond 1 TeV is still compatible with these search limits. The bounds coming from precision electroweak observables [25] and LHC direct searches for a heavy top-like quarks rule out any heavy quark below 600 GeV [25–27]. These searches for heavy Higgs as well as heavy top partners are carried out independent of each other. Thus, even if there is a discovery in any of these search modes, it is difficult to pin-point the right class of model. The aim of this paper is to present a unified search strategy for the heavy Higgs scalar and the heavy top-partner. This would eventually serve as a litmus test in distinguishing models belonging to Class-A from Class-B.

Model: Consider a simplified model with a heavy Higgs-like scalar (H_1) and a vector-like gauge

singlet fermion (t'). The relevant couplings of the scalar H_1 to t', gluons[1] and third generation quarks are governed by the following effective Lagrangian:

$$\mathcal{L}_{eff} \supset G^a_{\mu\nu} G^a_{\mu\nu} H_1 + \left(Y_t \bar{Q}_3 H_1 t' + Y_t \bar{Q}_3 H_1 t + h.c. \right) \tag{1}$$

where $G^a_{\mu\nu}$ is the field strength tensor for the gluons. We have assumed the rest of the vector-like spectrum to heavy and it gets decoupled from the low energy theory. Without loss of generality, we assume the coupling strength of the scalar H_1 to Q_3 and t' to be the same as Y_t, the top Yukawa coupling. Since the heavy scalar H_1 has Higgs-like interaction, its decay to a pair of $t\bar{t}, WW, ZZ, hh$ is common for both classes of models under consideration. As mentioned earlier, models belonging to Class B are characterized by the presence of an additional vector-like states. In the minimal setup, the interaction Lagrangian for a top partner t' is given as

$$\mathcal{L}_{t'th} \supset Y_t \bar{Q}_3 H \bar{t}' + M_{t'} \bar{t}' t \tag{2}$$

The first term in Eq. 2 induces a mass-mixing between the SM top and its vector-like counterpart. In the presence of this mixing the mass-basis is related to the interaction basis as:

$$\begin{bmatrix} t_1 \\ t_2 \end{bmatrix}_{L,R} = \begin{bmatrix} c_\theta & -s_\theta \\ s_\theta & c_\theta \end{bmatrix} \begin{bmatrix} t \\ t' \end{bmatrix}_{L,R} \tag{3}$$

where t_1 is now identified as the SM top and t_2 is the heavier partner. θ is the angle of rotation to move from the interaction basis to the mass basis. Henceforth, the top will be denoted as t for convenience. The presence of an additional fermion t_2 opens up an additional channel for H_1 to decay i.e $H_1 \to t t_2$. For the setup under consideration in Eq.2, t_2 can only decay into $t\ (b)\ +\ X$ where $X = W, h, Z$. The branching fraction of t_2 decaying to the gauge bosons is governed by its interaction to the scalar degrees of the Higgs doublet H. Two out of four degrees of freedom correspond to the longitudinal polarization of $W^\pm$, while one is that of the Z-boson. The remaining is the SM Higgs boson h. Consequently, one can roughly estimate the branching rates to be

$$B.R(t_2 \to b + W) \sim 50\%; \;\; B.R(t_2 \to t + h) \sim 25\%; \;\; B.R(t_2 \to t + Z) \sim 25\% \tag{4}$$

All the channels corresponding to $H_1 \to t t_2 \to t t(b) X$ as depicted in Fig. 1 are characterized by distinct kinematic endpoints in certain invariant mass distributions. This unique feature not only distinguishes it from SM backgrounds, but also from models belonging to Class A, serving as

[1] H is assumed to be produced through gluon fusion diagram with SM top quarks propagating in the loop

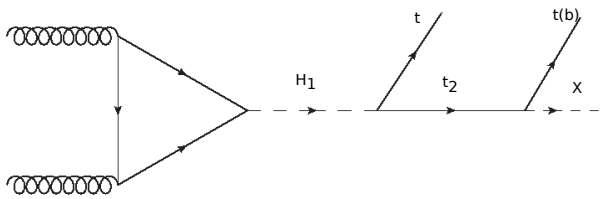

FIG. 1: *ggF production of H_1 and its decay to t t(b) X*

a smoking gun signal for Class B. We now study each of these channels and define the invariant mass distributions where the kinematic endpoints can be observed.

Channel 1 - $H_1 \to tt_2 \to tbW$

This is the most dominant channel where H_1 decays to t and t_2 with t_2 further decaying to b -quark and W-boson. While the top decays hadronically, we consider the leptonic decay mode W- boson. The topology is endowed with the following features:

- **Kinematic edge in the m_{bt} distribution:** The invariant mass distribution of the top and bottom quarks system is characterized by a kinematic endpoint [28] which is given as

$$\left(m_{tb}^{edge}\right)^2 \;=\; m_t^2 \;+\; m_b^2 \;+\; 2\left(E_t E_b - \mathbf{P}_t.\mathbf{P}_b\right) \tag{5}$$

  where t is the top quark originating from the heavy Higgs while the b-quark emerges from the decay of t_2. The magnitude of the quarks momentum in the rest frame of t_2 are given as

$$\begin{aligned} p_t^2 &= \frac{m_t^4 + m_{t_2}^4 + m_{H_1}^4 - 2\left(m_t^2 m_{t_2}^2 + m_t^2 m_{H_1}^2 + m_{t_2}^2 m_{H_1}^2\right)}{4m_{t_2}^2} \\ p_b^2 &= \frac{m_{t_2}^4 + m_b^4 + m_W^4 - 2\left(m_b^2 m_{t_2}^2 + m_b^2 m_W^2 + m_{t_2}^2 m_W^2\right)}{4m_{t_2}^2} \end{aligned} \tag{6}$$

  and $E_i^2 = m_i^2 + p_i^2$. The invariant mass acquires its maximum value when the angle between the top quark and the bottom quark is π. The edge of the invariant mass is a function of the mass of H_1 and t_2. Right panel of Fig. 2 gives the position of the edge in the m_{tb} distribution as a function of m_{t_2}. It is plotted for two different masses of the heavy scalar H_1. The green curve represents the edge for $m_{H_1} = 1100$ GeV and the blue curve is for 1200 GeV.

  It is clear from Fig. 2 that the position of the edge is unique to the choices of masses under consideration. At this stage it is important to note that we are limited in our choices for the masses for these two particles. Due to s-channel suppression, the production cross section of the heavy Higgs falls rapidly with increase in mass. Reducing it will necessitate reducing the

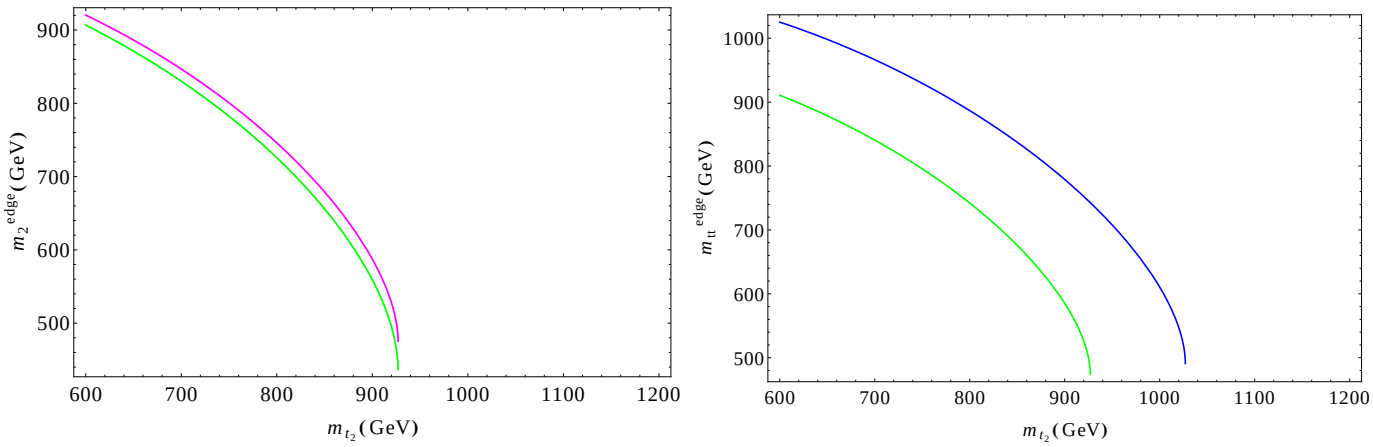

FIG. 2: *Variation of the edge of invariant mass for two final state quarks with mass of t_2 (left figure). The green plot represents the edge for $H_1 \to tbW$ and magenta plot is for $H_1 \to tth$. Variation of the edge of m_{tb} with mass of t_2 (right figure) for H_1 having mass of 1.1 TeV (green) and 1.2 TeV (blue).*

mass of vector-like quark (m_{t_2}) putting it in tension with the searches for third generation vector-like quarks. Thus, we consider the following two benchmark points:

$$\begin{aligned} \text{B1}: \; m_{H_1} &= 1.2 \text{ TeV}, \; m_{t_2} = 600 \text{ GeV}; \\ \text{B2}: \; m_{H_1} &= 1.1 \text{ TeV}, \; m_{t_2} = 700 \text{ GeV}. \end{aligned} \tag{7}$$

The parton-level distribution for m_{tb} is given in the left panel of Fig. 3. Clearly, the distribution exhibits a kinematic edge for both the benchmark points in Eq. 7. Right panel of Fig. 3 shows the corresponding distribution for m_{bl}.

- **Kinematic edge in the m_{lb} distribution:** In addition to m_{tb}, the invariant mass distribution of the bottom quark and the lepton also exhibits distinct edge given by

$$\left(m_{bl}^{edge}\right)^2 = m_b^2 + 2\left(E_b E_l + |\mathbf{P}_b||\mathbf{P}_l|\right) \tag{8}$$

where the lepton (l) originates from the W decay. The magnitude of the quarks momentum in the rest frame of W are given as

$$p_l^2 = \frac{m_W^2}{4} \; , \; p_b^2 = \frac{m_{t_2}^4 + m_b^4 + m_W^4 - 2\left(m_b^2 m_{t_2}^2 + m_b^2 m_W^2 + m_{t_2}^2 m_W^2\right)}{4m_W^2} \tag{9}$$

and $E_i^2 = m_i^2 + p_i^2$.

- **Kinematic edge in m_{tbl} distribution:** For completeness, we also note that the invariant mass of top, bottom and lepton system also shows behaviour similar to m_{tb} and m_{bl}. The

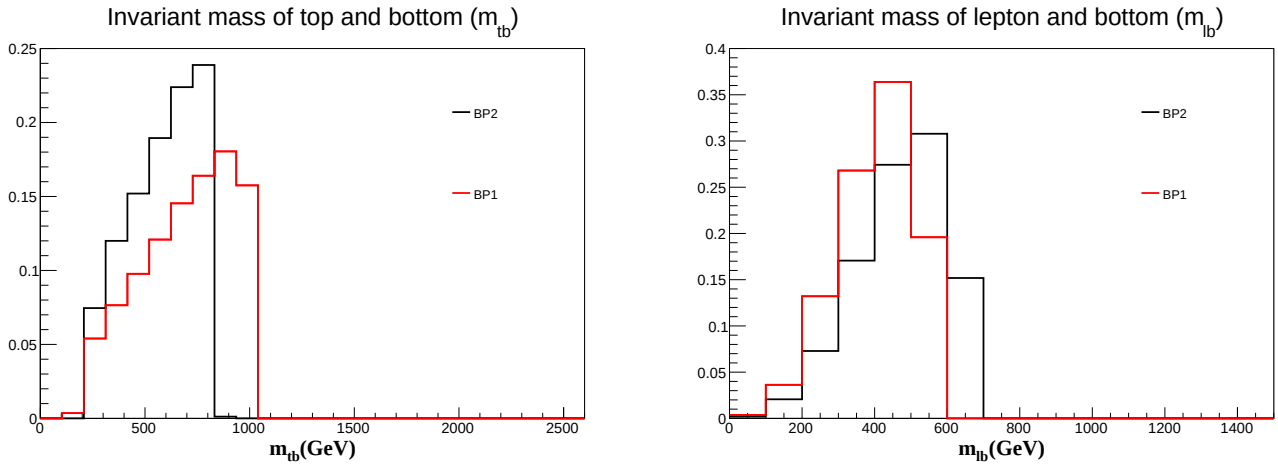

FIG. 3: *Parton-level distributions for m_{tb} (left) and m_{lb} (right) for the two benchmark points, BP1 (red) and BP2 (black)*

distribution has an edge at mass of the heavy resonance i.e. m_{H_1}. The distribution does not reveal any further information which can add to ones obtained from m_{tb} and m_{bl} and hence, will not be considered further.

The parton-level plots in Fig 3 are generated by implementing the Lagrangian given in Eq. 1 and 2 in FEYNRULES [29] and interfacing it with MADGRAPH [30]. Substitution of the masses in Eq. 5 gives m_{tb}^{edge} at 840 GeV which is roughly the location of the edge in the plot. Given the fact that we are restricted in our choice of the masses for the heavy resonances, Fig 2 can be used to determine the masses of H_1 and t_2 exclusively. The mass of t_2 determined from Fig 2 can be validated by plotting m_{bl} (right panel of Fig 3), which has a kinematic endpoint at m_{t_2}.

The presence of such kinematic edges is unique to cascade topologies of the form in Fig. 1. This feature has been used extensively in SUSY searches [31] for heavy neutralino χ_2^0 (equivalent to H_1 in Fig. 1), which decays into a di-lepton pair (equivalent to pair of quarks in Fig. 1) and missing energy χ_1^0 (equivalent to X). Unlike SUSY, however, the known masses of the final state particles increases the utility of this variable to a far greater effect.The combinations of the invariant mass in this channel are bereft of combinatorial uncertainties that are typical in SUSY and other channels discussed below.

There exists a very minute possibility of m_{tt} edge being possible in MSSM due to the following topology:$\tilde{g}\tilde{g} \rightarrow tttth$. Here the $\tilde{t}_1$ and t are nearly degenerate resulting in extremely light neutralinos. However, this is beset with a combinatorial uncertainty which will significantly smear the presence of an edge. In addition, the presence of a complimentary edge in m_{bl} discounts this

possibility as sbottoms degenerate with bottom mass is not possible.

Channel 2 - $H_1 \to tt_2 \to ttZ$

We consider leptonic decay of Z-boson while both the tops decay hadronically. Similar to the Channel 1, this mode also exhibits the following features:

- **Kinematic edge in the m_{tt} distribution:** The distribution of the invariant mass of the top pairs has an edge given by [2].

$$\left(m_{tt}^{edge}\right)^2 \;=\; 2m_t^2 \;+\; 2\left(E_{t_a}E_{t_b} + |\mathbf{P}_{t_a}||\mathbf{P}_{t_b}|\right) \tag{10}$$

  The magnitude of the transverse momenta of the top quarks in the rest frame of t_2 is given by

$$\begin{aligned} p_{t_a}^2 &= \frac{m_t^4 + m_{t_2}^4 + m_{H_1}^4 - 2\left(m_t^2 m_{t_2}^2 + m_t^2 m_H^2 + m_{t_2}^2 m_{H_1}^2\right)}{4m_{t_2}^2} \\ p_{t_b}^2 &= \frac{m_t^4 + m_{t_2}^4 + m_h^4 - 2\left(m_t^2 m_{t_2}^2 + m_t^2 m_h^2 + m_{t_2}^2 m_h^2\right)}{4m_{t_2}^2} \end{aligned} \tag{11}$$

  where $t_{a,b}$ are the two tops for the event and $E_i^2 = m_i^2 + p_i^2$.

Channel 3 - $H_1 \to tt_2 \to tth$ We consider $h \to b\bar{b}$ decay mode of the Higgs as it is the most dominant. The final states is characterized by a pair of top and bottom quarks. We consider one of the tops to decay semi-leptonically that suppresses multi-jet QCD background. Similar to Channel 2 this topology also exhibits a kinematic edge in m_{tt} distributions as well as the transverse mass M_T of the t, h system.

While the parton-level results are all promising, it is still challenging to observe the edges at the LHC beneath the SM backgrounds with proper identification of the top, bottom and Higgs.The rest of the analysis is dedicated in identifying a collider strategy which can closely reproduce the parton-level plots in Fig. 3.

Identifying edges at the LHC

The final state particles in a collider environment are typically identified in terms of leptons, photons, τ and jets. The strength of the analysis lies, not only in reproducing the parton-level plots presented earlier but also in its effectiveness in reducing the SM backgrounds. In a scenario

[2] The distribution of the invariant mass of the top quark which is the daughter of t_2 and one of the leptons will also have the kinematic edge similar to m_{lb}. However, unlike m_{lb} the identity of top is uncertain and leads to a combinatorial uncertainty. Additionally, the transverse mass of top quark and Z-boson defined by $m_T = \sqrt{m_Z^2 + m_t^2 + 2\left(E_T^t E_T^Z - \mathbf{p}_T^t.\mathbf{p}_T^Z\right)}$ also has an edge at m_{t_2}.

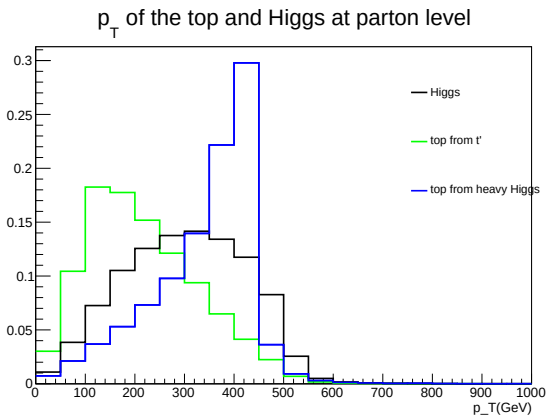

FIG. 4: p_T distribution of the top and the Higgs at the parton-level.

where top quarks, Higgs, Z and W-bosons are boosted, their decay products can be captured inside a cone of radius R. The criterion to determine R follows from the fact that the the mass difference between the heavy Higgs H_1 and the top partner t_2 must be significantly greater than the top threshold. i.e

$$\Delta m = m_{H_1} - m_{t_2} \geq 400 \text{ GeV}, \tag{12}$$

This ensures that the opening angle (R) between the top decay products is

$$R \sim \frac{2m_t}{p_T^t} \leq 1.5 \tag{13}$$

The specific choice of our benchmark points 7 warrants us such opening angle. Fig 4 shows the p_T distribution of the top quarks and the Higgs for Channel 3 with the second benchmark point. The p_T distribution has a peak at about 350 GeV for the leading top and the Higgs. As a result, the top jet, satisfies the condition in Eq.13. The Higgs, on account of its lighter mass will also satisfy the criterion in Eq. 13. The slightly larger choice of R ensures that the constituents of the sub-leading top can be captured inside a jet as well.

Jet Reconstruction: The parton-level events for our signal topology are generated with `MADGRAPH` at 14 TeV centre of mass energy using PDF `NNLO1` [32] The events are showered and hadronized using `PYTHIA` [33]. The showered events are then subsequently passed through the `DELPHES` detector simulator using the CMS card. We extract the calorimetric four vectors for each event using the following acceptance criteria:

$$E_{e-cal} > 0.1 \text{ GeV} \quad ; \quad E_{h-cal} > 0.5 \text{ GeV} \tag{14}$$

These calorimetric outputs are clustered using FASTJET [34] with the $Cambridge - Achen$ algorithm [35, 36] to reconstruct fat-jets. The top candidates in the event are identified using substructures of the reconstructed fat-jets with the jet reconstruction parameter to be $R = 1.5$. On account of the large transverse-momentum (p_T) associated with each event, we require the jet to have a minimum p_T of 50 GeV. The reconstructed 'fat' jets are required to have rapidity in the range $[-2.5, 2.5]$.

All the Channels discussed above are characterized by the presence of at least one top [3]. There has been tremendous improvement in the techniques of identifying boosted tops using TopTagger [37, 38]. We briefly outline the algorithm adapted by us for tagging the top jet;

- Scanning through the three leading jet in each event, we identify the top candidate using HEPTOPTAGGER [37].
- The fat-jets passing through the tagger are subject to filtering procedure where the constituents of each jet are reclustered with $R_{filt} = 0.3$.
- Out of all the subjets inside a jet, only $5(n_{filt})$ of the hardest subjets are retained.
- The invariant mass of the three subjets are required to lie between 150 GeV to 200 GeV.

We now discuss the individual strategy adapted for each of the decay channel of the t_2:

• $pp \to H \to tt_2,\ t_2 \to bW$: The three leading jet in the event correspond to one of the top, $b-$ jet and the $W-$ jet. Only events with a single isolated lepton associated with the decay of W-boson are selected. The leptons are isolated with respect to the fat-jets. For each event with a single lepton(at the parton-level), we construct a cone of $\Delta R = 0.3$ around the lepton. The leptons are considered to be isolated if the total energy deposit within this cone is less than 10% of the transverse momentum of the lepton. Since we assume the W to decay leptonically, the $W-$ jet can be easily differentiated from the other two by computing the hadronic energy fraction inside the jet defined as

$$\theta_J = \frac{1}{E_j^{total}} \sum_i E_i^{h-cal} \tag{15}$$

E_j^{total} is the total energy of the j^{th} jet and E_i is the energy deposited in the i^{th} $h - cal$ cell by a constituent of the j^{th} jet. A $W-$ like jet is likely to deposit all its energy in the electromagnetic calorimeter, θ_J is likely to be close to zero. On the other hand, top-like and $b-$ jets deposit

[3] In Channels 2 and 3 with two tops, only the leading top is tagged using the top tagger.

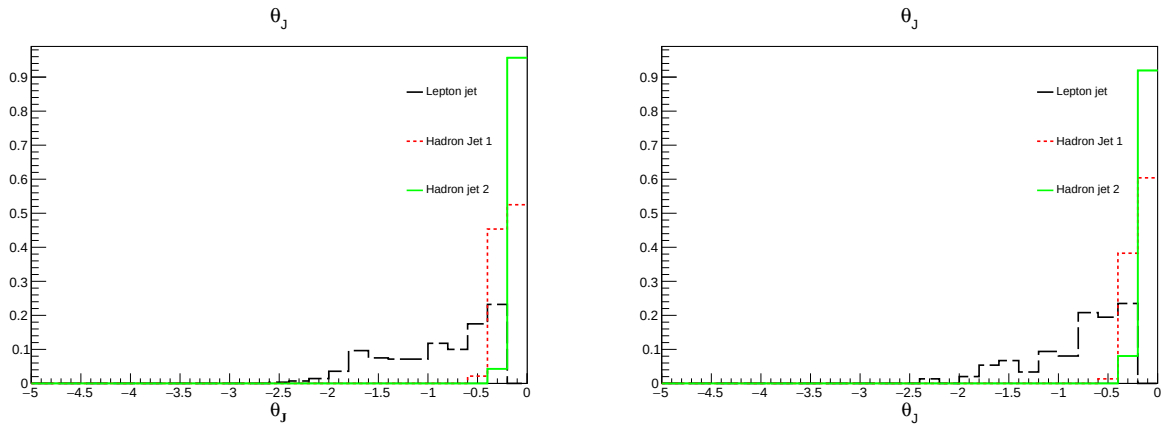

FIG. 5: θ_J *distribution for the three leading jets for Channel 1 (left) and Channel 2 (right)*

most of their energy in the hadronic calorimeter (since we consider hadronic decay of top). This leads to larger values of θ_J for them. It is convenient to take the logarithm of θ_J which further accentuates the difference between jet with or without hadronic activity. We identify W-like jet as the fat-jet having minimum hadronic activity. The other two jets are top-like jet and b-like jet. The distribution plotted in the left panel of Fig. 5 shows the comparison of $Log(\theta_J)$ of $W-$ like jet and the other hadronic jets (labeled as Hadron Jet 1(2)) for Channel 1.

As expected, $Log(\theta_J)$ for top-like and $b-$ jets peaks close to zero, while those for $W-$ like jet are large and negative in comparison. The presence of hadronic activity inside a $W-$ like jet can be attributed to the fact that these are fat ungroomed jets and are likely to collect stray QCD activity. After the identification of the $W-$ jet we identify the top from the remaining jets through top-tagger discussed above, while the remaining jet is considered to be the $b-$ jet. We find that a cut of $Log(\theta_J) < -0.5$ on the jet identified as the $W-$like is useful in suppressing the $t\bar{t}$ + jets background.

The distribution of the invariant mass of the lepton along with the jet not tagged as the top is plotted in the right panel of Fig. 6. Using the edge of m_{lb}, we can determine the mass of t_2. The distribution of the invariant mass of the two completely hadronic jets is given in the right panel of Fig.6. Both these distributions are plotted with 150 signal points. Similar distributions can be obtained for much lesser signal points. The position of the edge using monte-carlo simulation closely replicates that obtained using the parton-level information, thus highlighting the strength of our analysis.

- $pp \rightarrow H \rightarrow tt_2,\ t_2 \rightarrow tZ$: This channel is characterized by the presence of two top

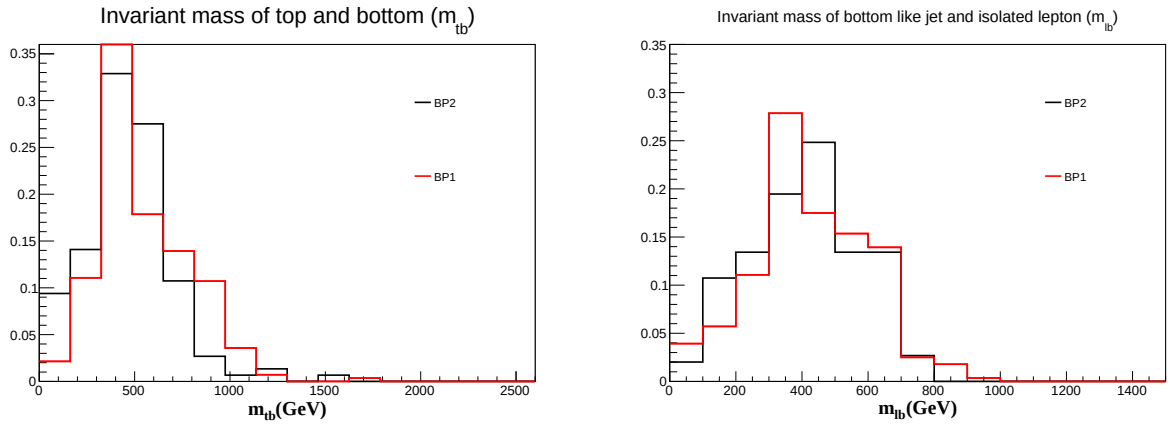

FIG. 6: *The simulation plots for m_{tb} (left) and m_{bl} (right) for the two benchmark points.*

quarks which decay hadronically along with the presence of a Z boson which is assumed to decay leptonically. The event is triggered by the presence of two isolated leptons. The Z jet can be distinguished from the top jet by computing the hadronic energy fraction inside the jet described above. The right panel of Fig. 5 shows the comparison of $Log(\theta_J)$ of $Z-$ like jet and the other hadronic jets (labeled as Hadron Jet 1(2)) for Channel 2. Like earlier, we give a cut of $Log(\theta_J) < -0.3$ on the $Z-$jet This is followed by tagging one of the top out of the two remaining jets. The left panel of Fig. 7 shows the distribution of fat-jet multiplicity. Right panel of Fig. 7 represents the distribution of m_{tt} constructed out of the filtered hadronic jets (with relatively larger hadronic content). The distribution is plotted with 200 signal points. One of the jet is tagged as the top. The plots for both the benchmark points exhibit an edge close to the expected value.

• $pp \rightarrow H \rightarrow tt_2,\ t_2 \rightarrow bh$: The signal is characterized by the presence of two top jets and a Higgs jet. We assume $h \rightarrow b\bar{b}$ decay mode of the Higgs. Multi-jet QCD background can be suppressed by assuming that one of the top decays leptonically. As a result we select events with a single isolated lepton. Once a top is tagged, we scan over the other leading jets to tag the Higgs used the `MASSDROP`[39] tagger outlined below:

- For a given candidate fat-jet j, the last stage of clustering is undone and broken into two subjets j_1 and j_2 such that $m_{j_1} > m_{j_2}$.
- In the event of a significant mass drop, $m_{j_1} < \mu m_j$, with a not too asymmetric splitting, $y = \frac{min(p^2_{t_{j_1}}, p^2_{t_{j_2}})\Delta R^2_{j_1 j_2}}{m_j^2} > y_{cut}$, the jet j is considered to be tagged.

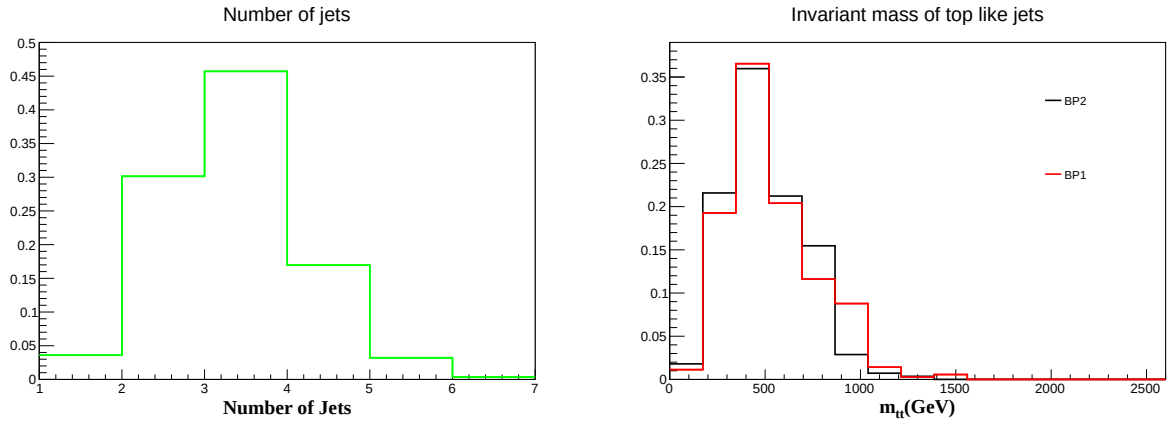

FIG. 7: Left panel shows the distribution of fat-jet multiplicity for channel 2 with BP1. Right panel corresponds to distribution of m_{tt} for this channel

- If the second condition is not satisfied, redefine j to be the subjet j_1 and first step is repeated.

μ and y_{cut} are real numbers and are chosen to be $\mu = 0.67$ and $y_{cut} = 0.09$. We retain only those 'Higgs-like jet' whose invariant mass lie within the window of 10 GeV centered about 125 GeV. The other top can be reconstructed by assuming neutrinos to be the only source of missing energy for the event. We extract transverse components of the neutrino momentum as the negative of the vector sum of the transverse momentum of all visible particles in an event. The z-component of the neutrino momentum is extracted by solving the equation for the W-boson mass $m_w^2 = (p_l + p_\nu)^2$ and is given as

$$p_{\nu z} = \frac{1}{2p_{eT}^2}\left(Dp_{eL} \pm E_e\sqrt{D^2 - 4p_{eT}^2 \not{E}_T^2}\right) \tag{16}$$

where $D = m_w^2 + 2\bar{p}_{eT}.\not{E}_T$ and we assume $D^2 - 4p_{eT}^2\not{E}_T^2 > 0$. Once the z-component of the 'neutrino' momentum is identified, we reconstruct W using the momenta of the isolated lepton and neutrino. We identify the anti-kt [40] b-tagged jet (reconstructed with $R = 0.5$ and $p_T^{min} = 50$ GeV) coming from the second top by demanding that ΔR between the Higgs-like jet (top-tagged jet) and the b-tagged jet is greater than 1.5. Using the b-tagged jet and W, we further reconstruct the semi leptonic top.

Fig 8 gives the m_{tt} distribution (in green) for the signal with the *ttbb* background superimposed (in blue). Both plots are plotted with about 35 signal points. The left plot shows a very distinct edge at ~ 800 GeV while the expected edge for $(m_H, m_{t_2}) = (1100, 700)$ is 839 GeV. Similar agreement is obtained for the mass combination $(m_H, m_{t_2}) = (1200, 600)$ where an edge-like feature is seen at 970 GeV while the parton-level result is at 1023 GeV. Thus our simulation can predict the location

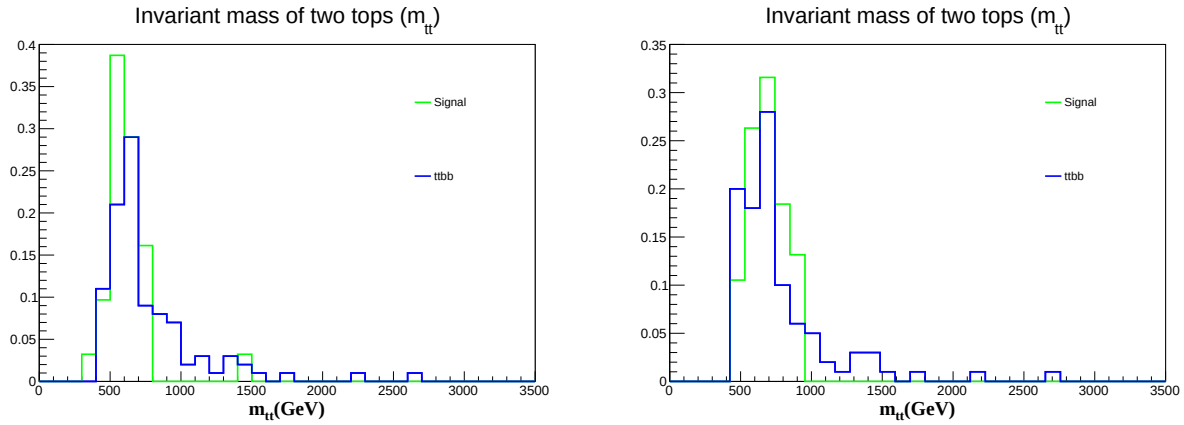

FIG. 8: m_{tt} distribution for signal (green) and $ttbb$ background (blue) for BP1 (right) and BP2 (left).

of the edges to within 10% of the actual value and can serve as a smoking gun for the existence of such topologies

Results and Discussion:

The observation of these distributions require certain number of signal events. In accordance with the branching fractions, we demand a minimum of $\sim$ 50,30,30 signal points for Channel 1,2 and 3 respectively. Table I gives the projected luminosities for the accumulation of these signal points for the calculated acceptance from our simulation. In computing the projected luminosities we assume 60% branching fraction of H_1 into tt_2. It also gives the predicted and the observed values of the edges for all three channels. The smaller efficiency for Channel 3 can be attributed to the fact that

	BP1(92 fb)				BP2(129 fb)			
Channel	Edge^{obs}	Edge$^{exp.}$	Efficiency	Luminosity(fb^{-1})	Edge^{obs}	Edge^{expec}	Efficiency	Luminosity(fb^{-1})
Channel 1(m_{tb})	$\sim$1000	1025	0.005	1100	$\sim$800	830	0.003	1300
Channel 2(m_{tt})	$\sim$1000	1036	0.007	$>$ 3000	$\sim$850	847	0.005	3000
Channel 3(m_{tt})	$\sim$970	1025	0.0008	$>$ 3000	$\sim$800	840	0.0008	3000

TABLE I: Reaches and predictions of the edges for three different channels. The cross-sections in brackets correspond to the gluon-gluon fusion production rate of the heavy resonance for the benchmark points at 13 TeV N^3LO.

in addition to the top tagging we also require the Higgs jet to be tagged. In addition the leptonic top is reconstructed from the b tagged jet which necessarily must not lie inside either of the top

tagged or the Higgs tagged jet. The efficiencies for the first two channels are on the lower side due to a cut on θ_J. Higher efficiencies can be obtained by either relaxing or completely ignoring the cut. However, this cut is highly essential in suppressing the $t\bar{t} + jets$ background which may possibly smear the edges. Channel 1 offers the most optimistic scenario for both the benchmark points observables at High Luminosity (HL) phase of the LHC. Additionally, this channel is free from any combinatorial uncertainties for the construction of the second edge (m_{lb}) which complements the m_{tb} distribution. Both these aspects make it an exciting prospect to explore. It is important to note that at this stage the cuts are not tuned to get the desired $S/\sqrt{B} \sim 5$ for the leptonic case. They are fashioned to get the desired kinematic distributions with enough signal points at much lower luminosities. Observation of these distributions would serve as a smoking gun to tighten the selection around the probable masses to achieve the desired significance.

We find that the analysis discussed thus far serves to achieve a two-fold objective: a) A definite pointer towards the existence of new physics scenarios. This, can be further extended to argue that it is an indicator towards the existence of non-MSSM scenarios. b) Gives a hint towards the region of parameter space where such new physics resonances can be expected to lie. An analysis of this nature has an extremely wide scope in general. Looking out for the existence of new physics by identifying characteristic unique to it can serve as a trigger which may aid the direct searches for the current and future runs.

Acknowledgements: We would like to thank Monoranjan Guchait and Tuhin Roy for useful discussions. We also thank N. Manglani for collaboration in the preliminary stages of the work. We would also like to thank Department of Theoretical Physics, TIFR for the use of its computational resources.

---

[1] K. Agashe, A. Delgado, M. J. May, and R. Sundrum, JHEP **08**, 050 (2003), hep-ph/0308036.

[2] T. S. Roy and M. Schmaltz, JHEP **01**, 149 (2006), hep-ph/0509357.

[3] C. Csaki, J. Heinonen, M. Perelstein, and C. Spethmann, Phys. Rev. **D79**, 035014 (2009), 0804.0622.

[4] S. Gopalakrishna, T. Mandal, S. Mitra, and G. Moreau, JHEP **08**, 079 (2014), 1306.2656.

[5] S. Gopalakrishna, T. Mandal, S. Mitra, and R. Tibrewala, Phys. Rev. **D84**, 055001 (2011), 1107.4306.

[6] A. De Simone, O. Matsedonskyi, R. Rattazzi, and A. Wulzer, JHEP **04**, 004 (2013), 1211.5663.

[7] R. Contino, L. Da Rold, and A. Pomarol, Phys. Rev. **D75**, 055014 (2007), hep-ph/0612048.

[8] N. Vignaroli, JHEP **07**, 158 (2012), 1204.0468.

[9] C. Anastasiou, E. Furlan, and J. Santiago, Phys. Rev. **D79**, 075003 (2009), 0901.2117.

[10] G. D. Kribs, A. Martin, and T. S. Roy, Phys. Rev. **D84**, 095024 (2011), 1012.2866.

[11] M. Carena, J. Hubisz, M. Perelstein, and P. Verdier, Phys. Rev. **D75**, 091701 (2007), hep-ph/0610156.

[12] T. Han, H. E. Logan, B. McElrath, and L.-T. Wang, Phys. Rev. **D67**, 095004 (2003), hep-ph/0301040.

[13] S. Matsumoto, T. Moroi, and K. Tobe, Phys. Rev. **D78**, 055018 (2008), 0806.3837.

[14] M. Buchkremer, G. Cacciapaglia, A. Deandrea, and L. Panizzi, Nucl. Phys. **B876**, 376 (2013), 1305.4172.

[15] A. Banfi, A. Martin, and V. Sanz, JHEP **08**, 053 (2014), 1308.4771.

[16] J. Li, D. Liu, and J. Shu, JHEP **11**, 047 (2013), 1306.5841.

[17] B. Gripaios, T. Mller, M. A. Parker, and D. Sutherland, JHEP **08**, 171 (2014), 1406.5957.

[18] M. Chala, J. Juknevich, G. Perez, and J. Santiago, JHEP **01**, 092 (2015), 1411.1771.

[19] M. Endo, K. Hamaguchi, K. Ishikawa, and M. Stoll, Phys. Rev. **D90**, 055027 (2014), 1405.2677.

[20] M. J. Dolan, J. L. Hewett, M. Krmer, and T. G. Rizzo, JHEP **07**, 039 (2016), 1601.07208.

[21] B. Dumont, J. F. Gunion, Y. Jiang, and S. Kraml, Phys. Rev. **D90**, 035021 (2014), 1405.3584.

[22] F. Mahmoudi, U. Maitra, N. Manglani, and K. Sridhar (2016), 1608.07407.

[23] G. Aad et al. (ATLAS), Eur. Phys. J. **C76**, 45 (2016), 1507.05930.

[24] G. Aad et al. (ATLAS), Phys. Rev. Lett. **113**, 171801 (2014), 1407.6583.

[25] S. A. R. Ellis, R. M. Godbole, S. Gopalakrishna, and J. D. Wells, JHEP **09**, 130 (2014), 1404.4398.

[26] G. Aad et al. (ATLAS), JHEP **08**, 105 (2015), 1505.04306.

[27] J. A. Aguilar-Saavedra, R. Benbrik, S. Heinemeyer, and M. Prez-Victoria, Phys. Rev. **D88**, 094010 (2013), 1306.0572.

[28] C. G. Lester, Phys. Lett. **B655**, 39 (2007), hep-ph/0603171.

[29] N. D. Christensen and C. Duhr, Comput.Phys.Commun. **180**, 1614 (2009), 0806.4194.

[30] J. Alwall, M. Herquet, F. Maltoni, O. Mattelaer, and T. Stelzer, JHEP **1106**, 128 (2011), 1106.0522.

[31] C. G. Lester, M. A. Parker, and M. J. White, JHEP **10**, 051 (2007), hep-ph/0609298.

[32] R. D. Ball et al., Nucl. Phys. **B867**, 244 (2013), 1207.1303.

[33] T. Sjostrand, S. Mrenna, and P. Z. Skands, Comput. Phys. Commun. **178**, 852 (2008), 0710.3820.

[34] M. Cacciari, G. P. Salam, and G. Soyez, Eur. Phys. J. **C72**, 1896 (2012), 1111.6097.

[35] Y. L. Dokshitzer, G. D. Leder, S. Moretti, and B. R. Webber, JHEP **08**, 001 (1997), hep-ph/9707323.

[36] S. Bentvelsen and I. Meyer, Eur. Phys. J. **C4**, 623 (1998), hep-ph/9803322.

[37] T. Plehn, G. P. Salam, and M. Spannowsky, Phys. Rev. Lett. **104**, 111801 (2010), 0910.5472.

[38] D. E. Kaplan, K. Rehermann, M. D. Schwartz, and B. Tweedie, Phys. Rev. Lett. **101**, 142001 (2008), 0806.0848.

[39] J. M. Butterworth, A. R. Davison, M. Rubin, and G. P. Salam, Phys. Rev. Lett. **100**, 242001 (2008), 0802.2470.

[40] M. Cacciari, G. P. Salam, and G. Soyez, JHEP **04**, 063 (2008), 0802.1189.